Automated Framework for the Augmentation of Missing Anatomical Structures and Generation of Personalized Atrial Models from Clinical Data

Luca Azzolin[1], Claudia Nagel[1], Deborah Nairn[1], Jorge Sánchez[1], Tianbao Zheng[1], Martin Eichenlaub[2], Amir Jadidi[2], Olaf Dössel[1], Axel Loewe[1]

[1] Institute of Biomedical Engineering, Karlsruhe Institute of Technology, Karlsruhe, Germany
[2] University Heart Center Freiburg-Bad Krozingen, Bad Krozingen, Germany

Abstract

Clinical and computational studies highlighted the role of atrial anatomy for atrial fibrillation vulnerability. However, personalized computational models are often generated from electroanatomical maps, which might lack important anatomical structures like the appendages, or from imaging data which are potentially affected by segmentation uncertainty. A bi-atrial statistical shape model (SSM) covering relevant structures for electrophysiological simulations was shown to cover atrial shape variability. We hypothesized that it could, therefore, also be used to infer the shape of missing structures and deliver ready-to-use models to assess atrial fibrillation vulnerability in silico. We implemented a highly automatized pipeline to generate a personalized computational model by fitting the SSM to the clinically acquired geometries. We applied our framework to a geometry coming from an electroanatomical map and one derived from magnetic resonance images (MRI). Only landmarks belonging to the left atrium and no information from the right atrium were used in the fitting process. The left atrium surface-to-surface distance between electroanatomical map and a fitted instance of the SSM was 2.26±1.95 mm. The distance between MRI segmentation and SSM was 2.07±1.56 mm and 3.59±2.84 mm in the left and right atrium, respectively. Our semi-automatic pipeline provides ready-to-use personalized computational models representing the original anatomy well by fitting a SSM. We were able to infer the shape of the right atrium even in the case of using information only from the left atrium.

1. Introduction

Atrial fibrillation (AF) is the most common sustained cardiac arrhythmia and is associated with high morbidity and mortality [1].

Computational models of the human heart built from clinical data have been used in in silico experiments to study arrhythmias and propose personalized treatments. However, the process of building a digital twin of a patient's heart directly from clinical geometrical data coming can be challenging since imaging data can be influenced by segmentation uncertainty and electroanatomical maps can be missing relevant anatomical structures (right atrium, appendage, veins).

Recently, a bi-atrial statistical shape model (SSM) covering the relevant anatomical variability required for in-silico electrophysiological experiments was presented and is generalizes well to unseen geometries [2].

Moreover, due to the complex myocardial structure, it is hard to reconstruct the atrial fiber direction and annotate the anatomical regions in an automated way.

In this work, we implemented an automated framework to augment missing anatomical structures and output a ready-to-use personalized computational model by fitting an SSM to the initial surface coming from clinical data, automatically label the different regions in the atria and compute the fiber orientation [3].

The pipeline was applied on a clinical dataset including both a geometry derived from MRI and an electroanatomical map.

2. Methods

2.1. Dataset

A high density electroanatomical bi-atrial map was taken in sinus rhythm prior to pulmonary vein isolation using a 20-pole mapping catheter and the CARTO 3 system (Biosense Webster Inc., Diamond Bar, CA, USA). Another bi-atrial geometry was derived by the segmentation of magnetic resonance images [4].

2.2. Rigid alignment and landmark generation

The atrial orifices (e.g. pulmonary veins, mitral valve in the left atrium) were automatically identified and labelled

using a clustering algorithm presented in [3]. The only landmarks required were the apex point of the atrial appendages. The surface mesh coming from clinical data was then pre-aligned to a bi-atrial SSM [2] using a rigid transformation matrix derived by minimizing the weighted sum of squared deviations between the atrial orifices centroids of the two surfaces. We decided to rigidly align in space before proceeding with the fitting to avoid a representation of translation and rotation parameters in the eigenmodes of the fitted SSM. The geometries used in this work were not included in the process of building the SSM. 35 characteristic points were automatically identified using geodesic paths connecting the previously marked orifices in the left atrium (10 in the pulmonary veins, 4 around the mitral valve ring, 4 in the roof, 2 in the septum, 1 in the left lateral wall, 9 in the anterior wall, 5 in the posterior wall) and used for the subsequent fitting procedure. If the left atrial appendage was present in the target geometry, a further landmark was added at the apex of the appendage.

2.3. Non-rigid shape model fit using Iterative Closest Points and Gaussian Process regression

We aimed to non-rigidly fit our SSM to a target surface using Iterative Closest Points (ICP) and Gaussian Process (GP) regression in order to establish correspondence between the two surfaces. This is different from the typical rigid ICP, which consists of finding the best rigid transformation between two meshes. Briefly, the main steps of the rigid ICP are the following: i) find candidate correspondences between the mesh to be aligned and the target by attributing the closest point on the target mesh as a candidate; ii) solve for the best rigid transform between the moving mesh and the target mesh using Procrustes analysis; iii) transform the moving mesh using this transformation; iv) repeat until we reach the limit number of iterations. The non-rigid ICP algorithm, which we used here for model fitting, performs the same steps. However, instead of finding a rigid transformation, it finds a non-rigid one using GP regression. The non-rigid transformation consists of the deformation that is encoded in the SSM eigenmodes. Given a set of points (in this case belonging to an instance of the SSM), we attribute the closest point on the target as a candidate correspondence to each of the points in the set. The returned sequence of points contains the candidate correspondences to the input points. The first main idea behind ICP is to use the candidate correspondences in a GP regression to find the best model instance explaining the observed deformations even though the correspondences are not perfect. We then defined a function that, when given a sequence of identifiers of model points and their candidate correspondence positions, computes a GP regression based on the resulting deformation field and returns the eigenmodes of the model instance fitting the candidate deformations best. These coefficients were then used as input to produce a bi-atrial geometry that fits our target LA. The non-rigid fitting of our SSM was implemented using ScalismoLab (`https://scalismo.org`).

2.4. Automated region annotation and fiber generation algorithm

Anatomical region annotation and fiber orientation calculations were performed using a highly automated pipeline based on a Laplace-Dirichlet-rule-based-method [3, 5]. The user interaction was further reduced by decreasing the number of required manually selected seed points from four to two (tip of left and right atrial appendage). The two additional landmarks needed previously on the left atrial appendage basis are now automatically identified by solving an additional Laplace equation using openCARP [6]. The algorithm was further improved by including the option of generating a bilayer model [7] in the case that only an endocardial surface mesh is given.

2.5. SSM fitting quality measures

The quality of the SSM fitting to the target clinical map was evaluated by computing the surface-to-surface distances using the *vtkDistancePolyDataFilter* (Kitware, Clifton Park, NY, USA).

3. Results and Discussion

The volume of the LA MRI segmentation was 80 mL and the corresponding best fitting instance had a blood pool volume of 75 mL. The original RA volume was 126 mL and the augmented RA that was obtained from fitting only the LA was 133 mL. We would like to recall that no information coming from the RA image was used to infer the RA mesh. Fig. 1 shows the result of the fitting procedure. We can notice how the fitted SSM instance represented the original MRI geometry very well, even using only few landmarks in the LA. The LA and RA computed surface-to-surface distances were 2.07 ± 1.56 mm and 3.59 ± 2.84 mm, respectively (Fig. 3). The average distance of 3.59 mm between the original segmentation and the inferred RA is remarkable if we think that we are in the range of less than 2 voxel diameters [8] omitting segmentation uncertainty. Regions with distances higher than 5 mm were located close to the inferior vena cava. This could be due to the incomplete segmentation of the vein's opening in the original manual segmentation.

The original electroanatomical map left atrium volume was 109 mL and the best fitted SSM instance resulted in a volume of 97 mL. The SSM fitted the left atrial wall very

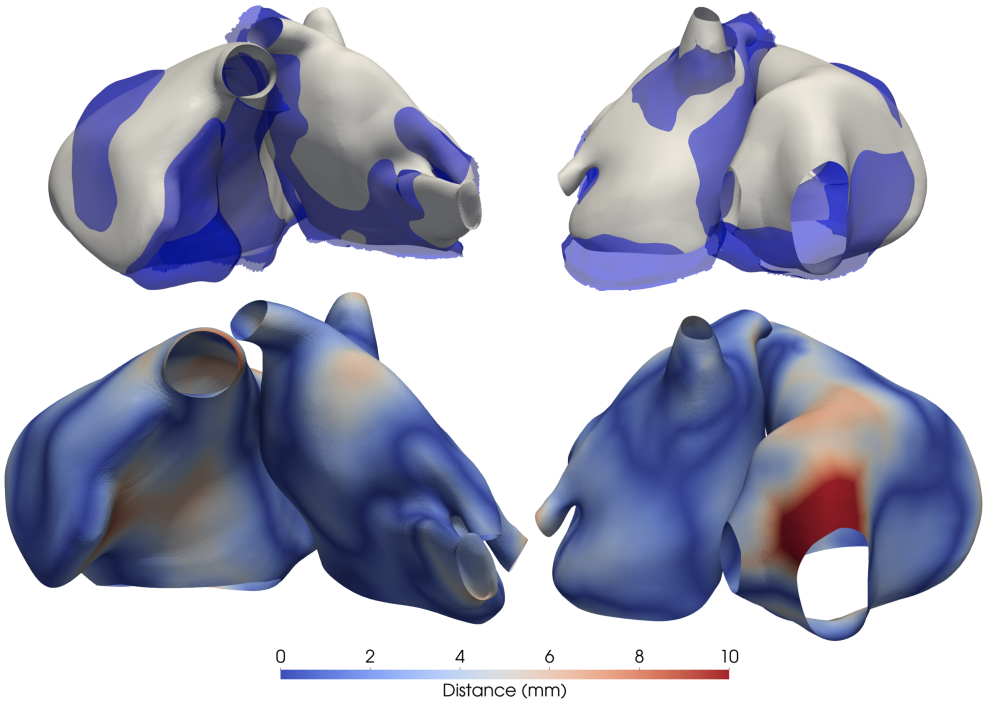

Figure 1. Top row: anterior (left) and posterior view (right) of the best fitting SSM instance (grey) to the target MRI segmentation (semi-tansparent blue). Bottom row: anterior and posterior view of the surface-to-surface distance between fitted SSM instance and target mesh shown on the fitted SSM instance.

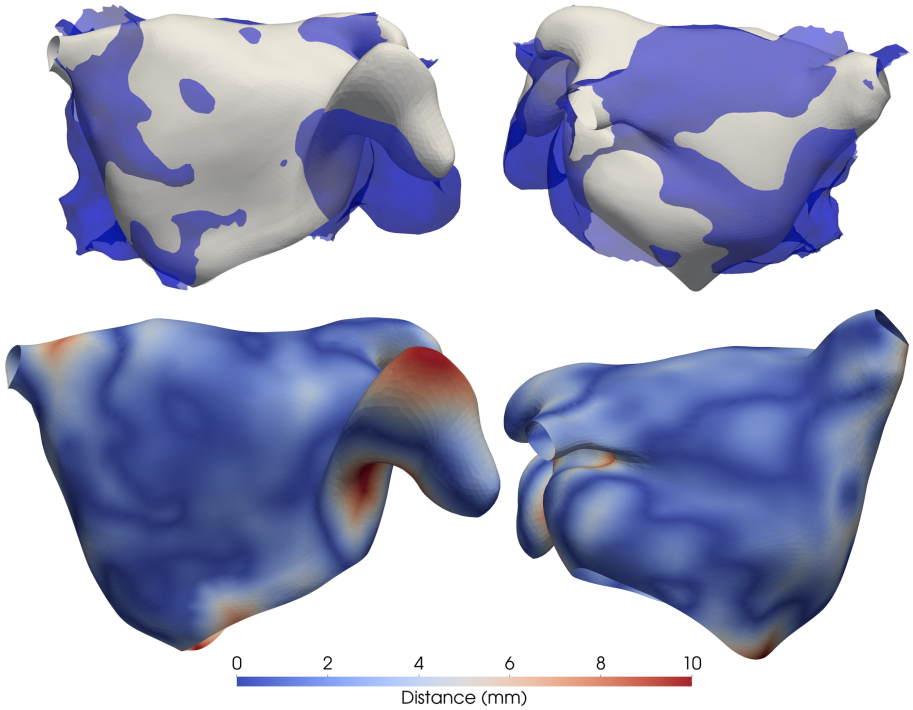

Figure 2. Top: anterior and posterior view of the SSM instance (grey) best fitting to the target CARTO electroanatomical map (semi-transparent blue). Bottom: anterior and posterior view of the surface-to-surface distance between the fitted SSM instance and the target mesh shown on the fitted SSM instance.

well (Fig. 2) even if the input anatomy had a lower quality compared to an MRI/CT segmentation. The surface-to-surface distance was 2.26±1.95 mm as shown in Fig. 3. Electroanatomical maps only partly cover the full volume of the left atrial appendage and therefore necessarily cause high surface-to-surface distances in that region.

The SSM was able to generalize well to unseen geometries and accurately represent important anatomical features including the left atrial volume. This work demonstrates a proof of concept on two example meshes. Performance on a bigger virtual population remains to be shown. Moreover, updating the SSM with more clinical data could further improve the patient-specific generalization in regions with high inter-individual variability such as as the appendages.

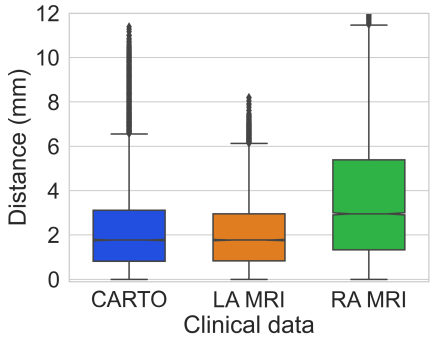

Figure 3. Surface-to-surface distances between the target mesh derived from clinical data (MRI or CARTO) and the corresponding fitted SSM. The RA mesh was purely inferred from the LA MRI landmarks and the SSM, no RA imaging data was used to inform the bi-atrial instance of the SSM.

4. Conclusion

We presented a semi-automatic pipeline that provides a ready-to-use personalized computational model by fitting a statistical shape model to a surface geometry obtained from clinical maps. The resulting augmented atrial model derived by the fitting algorithm represented the original anatomy very well and carefully reproduced the atrial volume even in the case of using only landmarks located in the left atrium to infer the right atrium.

Acknowledgments

This work was supported by European Union's Horizon 2020 research and innovation programme under the Marie Skłodowska-Curie grant agreement No.766082 (MY-ATRIA project), the EMPIR programme co-financed by the participating states and from the European Union's Horizon 2020 research and innovation programme under grant MedalCare 18HLT07, and by Deutsche Forschungsgemeinschaft (DFG) (project ID 391128822, SuLMaSS).

References

[1] Hindricks G, Potpara T, Dagres N, Arbelo E, Bax JJ, Blomström-Lundqvist C, Boriani G, Castella M, Dan GA, Dilaveris PE, Fauchier L, Filippatos G, Kalman JM, La Meir M, Lane DA, Lebeau JP, Lettino M, Lip GYH, Pinto FJ, Thomas GN, Valgimigli M, Van Gelder IC, Van Putte BP, Watkins CL. 2020 ESC guidelines for the diagnosis and management of atrial fibrillation developed in collaboration with the european association of cardio-thoracic surgery (EACTS). European Heart Journal 8 2020;.

[2] Nagel C, Schuler S, Dössel O, Loewe A. A bi-atrial statistical shape model for large-scale in silico studies of human atria: model development and application to ecg simulations. Medical Image Analysis 2021;102210.

[3] Zheng T, Azzolin L, Sanchez J, Dössel O, Loewe A. An automated pipeline for generating fiber orientation and region annotation of patient-specific atrial model. Current Directions in Biomedical Engineering 1 2021;1(1):409–412.

[4] Krueger MW, Seemann G, Rhode K, Keller DUJ, Schilling C, Arujuna A, Gill J, O'Neill MD, Razavi R, Dössel O. Personalization of atrial anatomy and electrophysiology as a basis for clinical modeling of radio-frequency ablation of atrial fibrillation. IEEE Trans Med Imaging 2013;32(1):73–84.

[5] Piersanti R, Africa PC, Fedele M, Vergara C, Dedè L, Corno AF, Quarteroni A. Modeling cardiac muscle fibers in ventricular and atrial electrophysiology simulations. Computer Methods in Applied Mechanics and Engineering 1 2021; 373:113468.

[6] Plank G, Loewe A, Neic A, Augustin C, Huang YL, Gsell MA, Elias Karabelas Mark Nothstein JS, Prassl AJ, Seemann G, Vigmond EJ. The openCARP simulation environment for cardiac electrophysiology. Computer Methods and Programs in Biomedicine 2021;208:106223.

[7] Labarthe S, Bayer J, Coudiere Y, Henry J, Cochet H, Jais P, Vigmond E. A bilayer model of human atria: mathematical background, construction, and assessment. Europace European Pacing Arrhythmias and Cardiac Electrophysiology Journal of the Working Groups on Cardiac Pacing Arrhythmias and Cardiac Cellular Electrophysiology of the European Society of Cardiology 1 2014;16 Suppl 4:iv21–iv29.

[8] Karim R, Blake LE, Inoue J, Tao Q, Jia S, Housden RJ, Bhagirath P, Duval JL, Varela M, Behar J, Cadour L, Van der Geest RJ, Cochet H, Drangova M, Sermesant M, Razavi R, Aslanidi O, Rajani R, Rhode K. Algorithms for left atrial wall segmentation and thickness - evaluation on an open-source CT and MRI image database. Medical image analysis 12 2018;50:36–53.

Address for correspondence:

Luca Azzolin
Fritz-Haber-Weg 1, 76131 Karlsruhe, Germany
publications@ibt.kit.edu